

# 18

## Deconvolution of $\Delta T$ profile curves

Olga Karousová\*

Miloš Karouš†

### 18.1 Introduction

At the present time, geomagnetic measurements are mainly carried out using proton magnetometers.

The modulus  $I$  of the total geomagnetic field is recorded, and the anomaly  $\Delta T = T - T_n$  is computed, where  $T_n$  is the modulus of the ambient Earth's total field. Since the anomaly is the algebraic difference between the absolute magnitudes of two generally non-parallel vectors, a quantity which lacks a direct physical interpretation, the interpretation of  $\Delta T$  anomalies brings some difficulties. For this reason measurements of the directional components of the geomagnetic field are sometimes carried out using other types of magnetometer, this happens particularly if a quantitative interpretation of the data is required.

For common surveying and preliminary prospecting, however, proton magnetometer measurements are sufficient. (There also exist methods of quantitative interpretation of  $\Delta T$  anomalies, but these are mostly suitable for the interpretation of anomalies above single magnetized bodies, and do not fit in the cases of interpretation of complex anomalies above composite geological bodies or a set of bodies of variable magnetization).

In this paper, a new interpretation method (or, more exactly, a transformation of  $\Delta T$  geomagnetic anomalies) is suggested, using digital deconvolution of profile values measured at equidistant points. In this method it is necessary to assume only induced magnetization or at least a magnetization in a known stable direction. Geological bodies irregular in shape with varying magnetic properties are divided into a set of elementary bodies of regular simple forms, such as plates or cylinders etc., at equal depths. In the interpretation, it is necessary to assume constant transversal dimensional (limited or unlimited) of the bodies, as well as in general the linear dependence of the anomaly on one sole parameter, be it a physical or a geometric one. Possible applications of the proposed method and its further advantages are discussed below.

### 18.2 The construction of the filter

Above simple bodies,  $\Delta T$  anomalies may be calculated analytically. The  $\Delta T$  anomaly above a horizontal infinitely elongated cylinder with its axis perpendicular to the profile  $x$  is given (Janovskij 1963, Logachev & Zacharov 1973, Lindner & Scheibe 1978)

---

\* Department of Applied Geophysics,  
Charles University,  
Prague,  
Czechoslovakia

† Department of Applied Geophysics,  
Charles University,  
Prague,  
Czechoslovakia

by

$$\Delta T^c(\xi) = \frac{2js \cos I_n}{(\xi^2 + h^2)^2} \{ (h^2 - \xi^2)(\tan^2 I_n - \cos^2 A) - 4h\xi \tan I_n \cos A \} \quad , \quad (18.1)$$

The relation for a vertical plate which has finite width, infinite horizontal length and infinite vertical extent (Logachev & Zacharov 1973) is

$$\Delta T^p(\xi) = 2b2J \frac{\cos^2 I_n}{\xi^2 + h^2} \{ h(\tan^2 I_n - \cos^2 A) - 2\xi \tan I_n \cos A \} \quad , \quad (18.2)$$

- where
- $j$  = magnetization
  - $I_n$  = inclination of induced magnetization (i.e. the dip of a normal magnetic field)
  - $A$  = azimuth of the profile, perpendicular to the elongation of the body
  - $h$  = depth of the upper margin of the plate or of the axis of the cylinder
  - $\xi$  = horizontal distance from the body's centre
  - $2b$  = width of the plate
  - $s$  = area of the vertical section of the cylinder

Let us designate as an amplitude function or parameter

$$D_a^c = J \cdot s \text{ for a cylinder} \quad (18.3)$$

and

$$D_a^p = 2b \cdot 2J \text{ for a plate} \quad (18.4)$$

Then it is possible to present the relations for the calculation of a  $\Delta T$  in the form:

$$\Delta T^c(\xi) = D_a^c \cdot R^c(\xi) \quad (18.5)$$

and

$$\Delta T^p(\xi) = D_a^p \cdot R^p(\xi) \quad , \quad (18.6)$$

where the functions  $R^c(\xi)$  and  $R^p(\xi)$  for the given body at a specified depth  $h$  depend on the parameters  $I_n$  (inclination),  $A$  (azimuth of the profile) and  $\xi$  (the horizontal distance from the centres of the bodies). For the given inclination  $I_n$  and azimuth  $A$ , the functions  $R$  depend only on the co-ordinates  $\xi$  giving the shape of the anomaly above a single body. We shall designate them as shape functions. The set of values  $R_i = R(\xi_i)$  of the digitised function  $R$  at the equidistant points  $\xi_i = \xi_o + i \cdot \Delta x$  ( $\Delta x$  is the digitisation step, while  $\xi_o$  is the beginning of digitisation) will be designated as filtration coefficients  $R_i$ .

The shape function is non-zero within a restricted interval, since for large distances  $\lim_{\xi \rightarrow \pm\infty} R(\xi) = 0$  is valid. Thus, the set of filtration coefficients forms a finite series.

The  $\Delta T$  anomaly above a system of equal bodies (having various parameters  $D_{aj}$  placed at equal depths  $h$  at points  $x_j = j \cdot \Delta x$ ) can be expressed in the form of a series where the spacing of both the data and the sources  $\Delta x$  is the same;

$$\Delta T(x_i) = \sum_{j=m}^n D_{aj} \cdot R(x_i - x_j) \quad (18.7)$$

If we use the notation  $\Delta T(x_i) = T_i$  and  $R(x_i - x_j) = R_{i-j}$ , then the relation (18.7) takes on the form of a digital convolution:

$$T_i = \sum_{j=m}^n D_j \cdot R_{i-j} \quad (18.8)$$

Similarly,  $\Delta T$  anomalies above a set of equal bodies of arbitrary shape may be expressed in the form of digital convolution. Relation (18.7) may be written in the symbolic shortened form:

$$T = D_a * R, \quad (18.9)$$

where the symbol  $*$  represents convolution multiplication, and its meaning is expressed by equation (18.8). A similar approach was used also by Bhattacharyya & Chan 1977.

Knowing the distribution of the amplitude parameter  $D$ , depending on the size of the body (for a cylinder of section  $s$  and for a plate of width  $2b$ ) as well as magnetization  $J$ , it is possible to calculate the  $\Delta T$  anomaly according to relation (18.8) or (18.9) by the linear filtration of distribution  $D$ . The total number of filtration coefficients  $R_i = R(\xi_0 + i \cdot \Delta x)$  is  $(n - m + 1)$ .

When the entire vertical section is divided into a set of elementary bodies (e.g. right parallelepipeds) of varying magnetization, filtration may enable the calculation of effect of the bodies at equal depths, and the total effect of the whole section then will be equal to the sum of the effects of the bodies at the individual depths. However, this approach is possible only if the principle of superposition is valid.

### 18.3 Deconvolution of $\Delta T$ profile curves

If we consider that a  $\Delta T$  anomaly in a profile is produced by a set of bodies of the same geometric shape but of different magnetization values (i.e. different amplitude parameters  $D$ ) we may determine the values of the parameters for the individual bodies placed at equidistant points from the measured anomalies by means of deconvolution. The inversion (deconvolution) relation is obtained from relation (18.9) by convolution multiplication with the inversion filter  $R^{-1}$ :

$$T * R^{-1} = D_a * R * R^{-1} \quad (18.10)$$

The inversion filter must fulfil the following condition, provided that  $R$  is nonsingular:

$$R * R^{-1} = \theta \quad (18.11)$$

where  $\theta$  is the convolution unit (or identity matrix) which has the property for an arbitrary series  $X$  that  $X = \theta * X$ . Equation (18.10) becomes

$$D = T * R^{-1}. \quad (18.12)$$

Equation (18.11) is valid for the computation of inversion coefficients  $R_j^{-1}$  of the deconvolution filter  $R^{-1}$ . But in general it leads to finding an infinitely long inversion filter which cannot be of practical significance. For a practical deconvolution it is necessary to use the so-called truncated filters with the final number of coefficients  $(N-M+1)$ . An equation for this deconvolution has the following form:

$$\bar{D}_i = \sum_{j=m}^N \bar{R}^{-1} \cdot T_{i-j}, \text{ i.e. } \bar{D} = T * \bar{R}^{-1}. \quad (18.13)$$



The set of equations (18.11) cannot be exactly fulfilled for the truncated filtration. Coefficients are regarded as optimal, which fulfil the set of equations so that the sum of squares of the deviations  $E = R^*R^{-1} - 0$  is a minimum. These are the least squares coefficients (Rice 1962, Kanasewich 1975). The outputs of the inversion filtration  $\bar{D}$  then differ from the actual distribution of the amplitude parameters  $D_i$ . The error depends on the digitisation step  $\Delta x$ , the shifting of digitisation points  $\xi_i$  and the position of bodies  $x_i$  - i.e.  $\xi_o = \xi_i - x_i$ , the number of inversion coefficients ( $N-M+1$ ), the number of filtration coefficients ( $n-m+1$ ), and of course, the form of the function  $R$ .

To minimise the value  $\sum E_i^2$ , we set its partial derivatives with respect to  $R^{-1}$  equal to zero. Now, the set of equations for the calculation of inverse least squares filters is as follows:

$$\sum_{j=m}^N \bar{R}_j^{-1} \cdot A_{k-j} = R_{-k} \quad (18.14)$$

where

$$A_k = \sum_{j=m}^n R_{j+k} \cdot R_j \quad (18.15)$$

where  $A$  is the autocorrelation of the filtration coefficients  $R$ .

A sufficient criterion for the correctness of the function of the derived deconvolution filter may be seen in the application of the filter to the anomaly above a known distribution of the amplitude parameter, best above a single magnetized body. The convolution of such an anomaly with a deconvolution filter should be nearly equal distribution of the actual parameter  $D_a$ .

#### 18.4 Deconvolution filters for a plate and a cylinder

Using the least squares method, deconvolution coefficients have been calculated for a horizontal cylinder and a thin vertical plate; in both cases the horizontal elongation of the bodies is infinite and perpendicular to the profile. For the calculation, the inclination  $I_n = 65^\circ$  has been chosen, which corresponds to a geomagnetic field at about  $50^\circ$  northern latitude. The coefficients have been calculated for four different azimuths of the profiles:  $A = 0^\circ, 30^\circ, 60^\circ$  and  $90^\circ$ . The last azimuth corresponds to vertical magnetization. The digitisation step  $\Delta x = h$  equal to the body depth has been verified empirically as most suitable.

As the number of the inversion filter coefficients is increased, the accuracy of the determination of the amplitude parameter  $D_a$  also rises. The mean square difference between the amplitude function and the deconvolution function  $E$  mostly decreases with the increasing length of the filter  $L = (N - M)\Delta x$  (Fig. 18.1). Filters as short as possible are advantageous on practical grounds, since in these the information loss on the margin of the profiles is rather small, and the computation is less time-consuming and less complicated. In this paper we used five- to nine-member filters (i.e.  $L = 4$  to 8). An example is given in Table 18.1: coefficients of an inversion (deconvolution) nine-member filter with a chosen digitisation step  $\Delta x = h$  for a vertical plate and a cylinder.

It is interesting that with increasing density of digitisation points, i.e. with decreasing digitisation step size, the precision of deconvolution does not in general increase. It can be shown by analysis in the frequency domain that a decreasing digitisation step corresponds to a shift in the maximum of the frequency spectrum of the function  $R$  to lower frequencies and, in contrast, leads to a shift in the deconvolution coefficients  $R^{-1}$  spectrum to higher frequencies. In the space domain this results

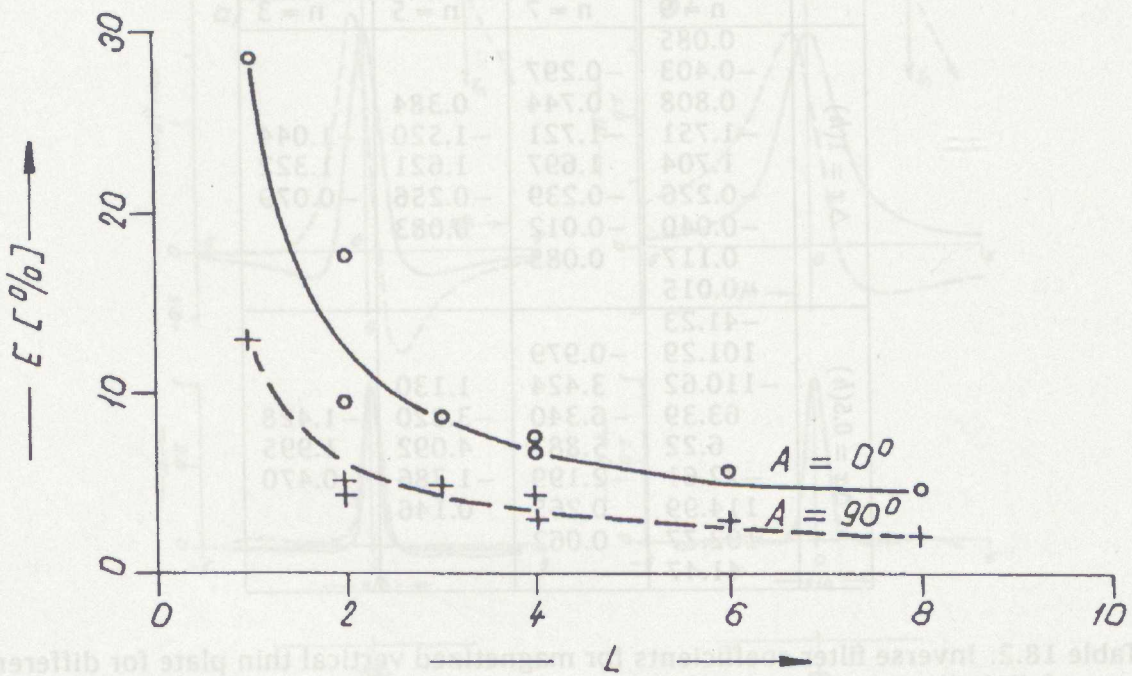


Figure 18.1: The mean square difference  $E$  between a real distribution of  $D$ -parameter and output of filtering  $D_a$  versus length of filter  $L$ .

Azimuth	$A = 90^\circ$	$A = 60^\circ$	$A = 30^\circ$	$A = 0^\circ$
horizontal cylinder	0.033	0.010	-0.006	-0.008
	0.041	0.014	-0.009	-0.022
	0.073	0.032	0.011	0.007
	0.005	-0.065	-0.142	-0.170
	0.624	0.586	0.491	0.454
	0.005	0.053	0.088	0.089
	0.073	0.100	0.094	0.093
	0.041	0.060	0.061	0.053
	0.033	0.050	0.053	0.049
vertical thin plate	-0.016	-0.002	0.044	0.085
	0.035	-0.160	-0.300	0.403
	0.151	0.410	0.664	0.808
	-0.936	-1.404	-1.654	-1.751
	2.097	2.009	1.791	1.704
	-0.936	-0.561	-0.324	-0.226
	0.151	0.084	0.049	-0.040
	-0.035	-0.016	0.003	0.117
	0.016	0.030	0.055	-0.015

Table 18.1: Inverse filter coefficients for a magnetized horizontal cylinder and vertical thin plate for different azimuths of profile  $A$ . Number of coefficients: 9



	n = 9	n = 7	n = 5	n = 3
$\Delta x = 1(h)$	0.085			
	-0.403	-0.297		
	0.808	0.744	0.384	
	-1.751	-1.721	-1.520	-1.044
	1.704	1.697	1.621	1.322
	-0.226	-0.239	-0.256	-0.079
	-0.040	-0.012	0.083	
	0.117	0.085		
	-0.015			
$\Delta x = 0.5(h)$	-41.23			
	101.29	-0.979		
	-110.62	3.424	1.130	
	63.39	-6.340	-3.820	-1.428
	6.22	5.882	4.092	1.995
	-72.61	-2.199	-1.386	-0.470
	114.99	0.265	0.146	
	-102.77	0.062		
	41.47			

Table 18.2: Inverse filter coefficients for magnetized vertical thin plate for different step of digitalisation  $\Delta x$  and different number of coefficients  $n$ .

in deconvolution coefficients with high absolute values and which alternate in sign causing the output deconvolution transformant  $D_a$  to alternate in sign as well. This produces lower stability of the filter. For the sake of comparison, in Table 18.2 values of deconvolution filters are given using a digitisation step of  $\Delta x = h$  and  $\Delta x = 0.5h$  for the plate.

### 18.5 Deconvolution curves

By linear filtration of  $\Delta T$  anomaly curves using nine-member deconvolution filters we obtain deconvolution transforms  $D$ . Fig. 18.2 illustrates  $\Delta T$  anomalies and deconvolution curves above a horizontal cylinder (a) and a vertical plate (b) calculated for inclination  $I_n = 65^\circ$  and for two extreme azimuths  $A = 0^\circ$  (dashed line) and  $A = 90^\circ$  (solid line), the two latter corresponding to vertical magnetization. In both these cases the deconvolution curves have their maxima only above the source of the anomaly, while in the surrounding points their values are almost zero. The difference from the actual distribution  $D$  of the parameter  $D_a$  is due to the finite length or the filter. The deconvolution curves are almost symmetrical even at the oblique inclined magnetization which is in contrast to  $\Delta T$  anomalies. From this point of view, the deconvolution transformation has a similar significance as reduction to the pole. But the deconvolution curves have a width which corresponds to that of the body if the influence of the digitisation step is neglected. Thus, maps of isolines of deconvolution transform  $D$  correspond better to a geological map than the isoline maps of original  $\Delta T$  anomalies. Owing to their small width,  $D$  curves also display better the separation capability, i.e. the capability to separate the effects of the near bodies. Fig. 18.3a shows  $\Delta T$  curves above two cylinders with different magnetizations (the magnetization of the righthand sphere is twice as high). Whereas the character of the  $\Delta T$  anomaly is asymmetrical with one maximum, the deconvolution curve  $D$  displays two maxima corresponding to effects of two different

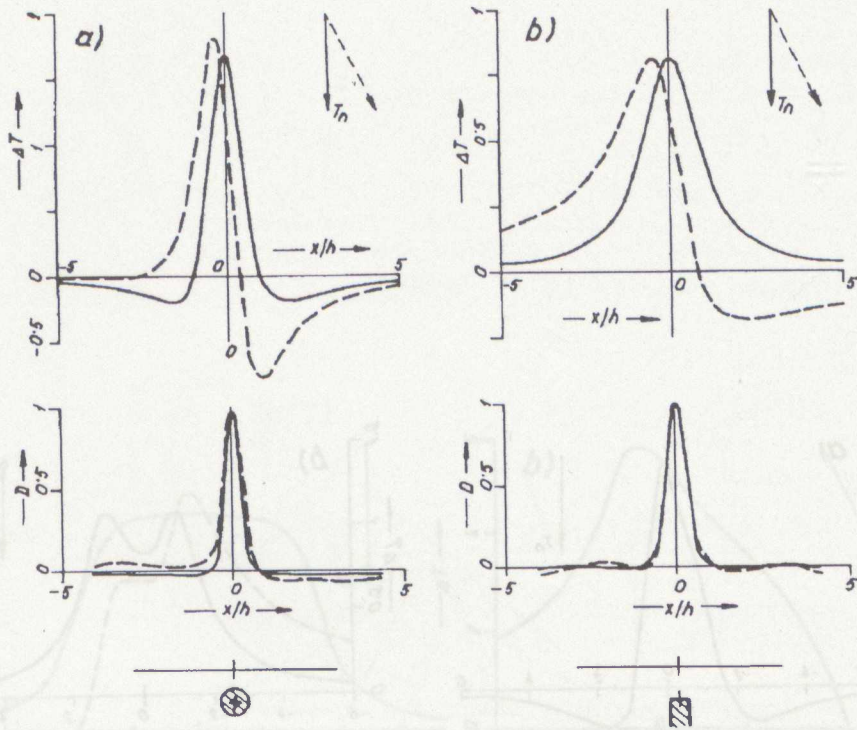


Figure 18.2:  $\Delta T$ -anomalies and deconvolution curves  $D$  above a magnetized a) cylinder and b) vertical plate.

bodies. The case of vertical plates magnetized vertically as well as obliquely is similar (Fig. 18.3b).

As it is possible to decompose a wide plate into a set of thin plates, the deconvolution transform  $D$  of a  $\Delta T$  anomaly above a wide plate gives a good idea of the horizontal limitation of the wide plate. A moderate asymmetry will appear in an inclined (oblique) magnetization (Fig. 18.4b), and by increasing the number of deconvolution coefficients we may approach an ideal result.

Deconvolution filters derived for vertical plates may also be used for transformation of  $\Delta T$  curves above dipping plates (Fig. 18.5). It is true that in this case the deconvolution curves are generally asymmetrical, but they are approximately equal in shape although the inclinations (directions) of magnetization are different. The steep gradients of the  $D$  correspond to the horizontal boundaries of the upper surface of the plates.

A practical example of the suggested method of deconvolution of the  $\Delta T$  profile curves is shown in Fig. 18.6. Magnetometry was used in archaeological prospecting for mapping two parallel ditches (probably pathway) in the neighbourhood of the village of Dřetkovice, central Bohemia. The area belongs to the known fortified hilltop-settlement Homolka—an industrial iron-smelting centre of the Řivnác early historical Roman culture. The fill of the ditches has a susceptibility which is a little higher than that of surrounding rocks. The measured  $\Delta T$  profile curves were deconvolution using a deconvolution filter for horizontal cylinders. The thickness of the ditches fill has been computed from the radii of the interpreted cylinders. The interpreted depths of the ditches according to magnetic prospecting correspond well to the depths as determined by excavation (Fig. 18.6d).



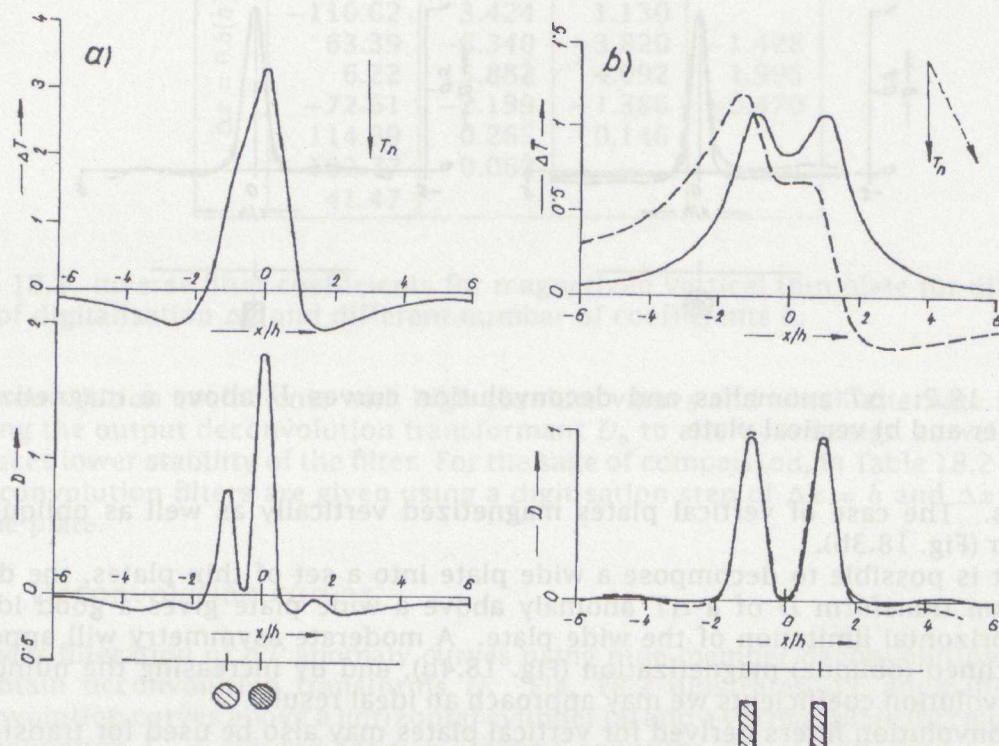


Figure 18.3:  $\Delta T$ -anomalies and  $D$ -curves above a) two cylinders with different magnetizations and b) above two vertical plates with equal magnetizations



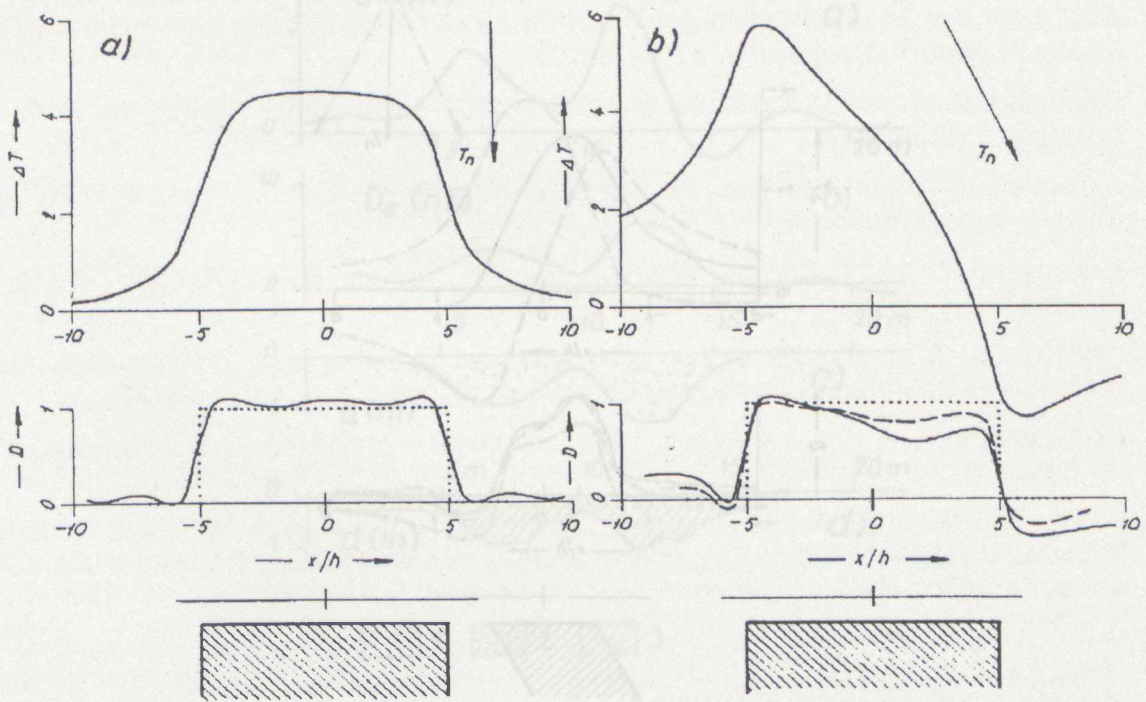


Figure 18.4:  $\Delta T$ -anomalies and  $D$ -curves above very wide plates for a) vertical and b) inclined magnetization

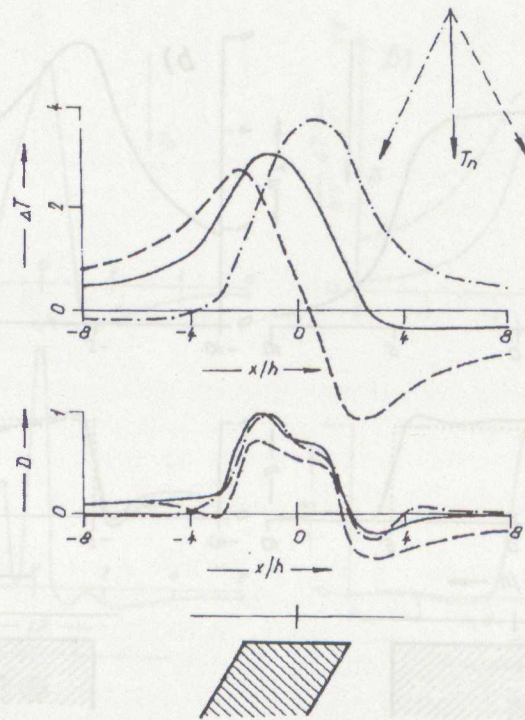


Figure 18.5:  $\Delta T$ -anomalies and  $D$ -curves above dipping plate for different inclination of magnetizing field



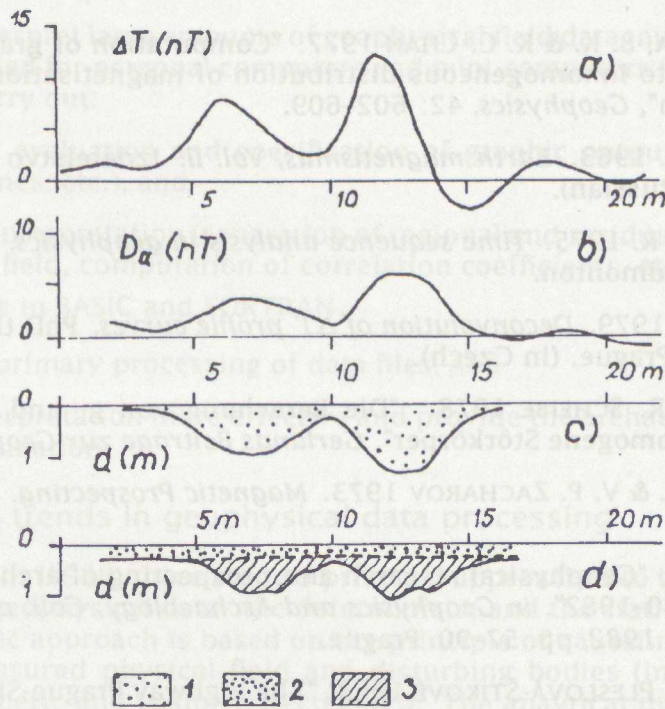


Figure 18.6: Magnetic profile along the double-ditch, locality Dřetovice: its deconvolution and interpretation. a)  $\Delta T$  profile curve, b) deconvolution curve, c) interpreted cross-section according to the magnetic measurements, d) cross-section as determined by excavation 1—interpreted ditches, 2—mould, 3—ditch fill

## 18.6 Conclusion

The method of deconvolution processing of  $\Delta T$  curves seems to be very promising for a preliminary elaboration of the data obtained by measurement using proton magnetometers, either in airborne or ground exploration. The advantage of an elaboration of this kind derives from its simplicity and source separation capacity. Maxima of deconvolution transforms  $D$  correspond to the position of the magnetized bodies. However, this method is applicable only in the case of a low magnetization for which the superposition principle may be assumed, and in the case of a known stable direction of magnetization in the profile, i.e. induced magnetization.

## Bibliography

BHATTACHARYYA, B. K. & K. C. CHAN 1977. "Computation of gravity and magnetic anomalies due to inhomogeneous distribution of magnetisation and density in a localized region", *Geophysics*, 42: 602–609.

JANOVSKIJ, B. M. 1963. *Earth magnetismus, Vol. II*. Izdatelstvo Leningrad. Univ. , Leningrad. (in Russian).

KANASEWICH, E. R. 1975. *Time sequence analysis in geophysics*. The University of Alberta Press, Edmonton.

KAROUSOVÁ, O. 1979. *Deconvolution of  $\Delta T$  profile curves*. PhD thesis, Fac. of Sci. , Charles Univ. , Prague. (in Czech).

LINDNER, H. & R. SCHEIBE 1978. "Die Berechnung von g- und T- Anomalien für regelmässige homogene Störkörper", *Gerlands Beiträge zur Geophysik*, 87.

LOGACHEV, A. A. & V. P. ZACHAROV 1973. *Magnetic Prospecting*. Nedra, Leningrad. (in Russian).

MAREK, F. 1983. "Geophysical research and prospecting of archaeological sites in Bohemia in 1980–1982". in *Geophysics and Archaeology; Coll. of Works of the 4th Symp. in Liblice 1982*, pp. 57–90. Prague.

MOUCHA, V. & E. PLESLOVÁ-ŠTIKOVÉ 1983. "The highway Prague-Slaný: The methodology and present results of advance rescue excavations". in *Geophysics and Archaeology; Coll. of Works of the 4th Symp. in Liblice 1982*, pp. 199–222. Prague.

RICE, R. B. 1962. "Inverse convolution filters", *Geophysics*, 27: 4–18.